Journal of Hydroscience and Hydraulic Engineering
Vol. 19, No.1 May, 2001, 117-130

FLOW TRANSITIONAL BEHAVIOR IN SMOOTH BED BOTTOM BOUNDARY LAYER BENEATH IRREGULAR OSCILLATORY MOTIONS

By

Mustafa Ataus SAMAD

Ph. D., Associate Specialist, Surface Water Modelling Centre, House 476, Road 32, New DOHS, Mohakhali, Dhaka 1206, Bangladesh, Email: samad@swmc.bangla.net

Hitoshi TANAKA

D. Eng., Professor, Dept. of Civil Engg., Tohoku Univ., Aobayama 06, Aoba, Sendai 980-8579, Japan, Email: tanaka@tsunami2.civil.tohoku.ac.jp

and

Hiroto YAMAJI

Laboratory Assistant, Ditto, Email: yamaji@kasen1.civil.tohoku.ac.jp

SYNOPSIS

Detailed flow measurements have been performed to investigate laminar-to-turbulent and turbulent-to-laminar transition in the bottom boundary layer under irregular oscillatory motions. Experimental data indicate that, apart from instantaneous flow properties, transitional behavior under irregular oscillatory motions is also affected by flow conditions in preceding oscillations. While laminar-to-turbulent transition requires a build-up of turbulent energy to initiate flow transition, during turbulent-to-laminar transition turbulent energy from previous higher oscillations carry over well into following smaller ones. Due to this 'History Effect' individual oscillations with much higher Reynolds numbers show laminar properties whereas oscillations with very small Reynolds number show transitional characters. Use of conventional transitional criteria from sinusoidal motions, therefore, becomes unsuitable to indicate flow transition under irregular oscillatory motions. Also transition occurs over a much wider range of Reynolds numbers than that observed for sinusoidal motions.

INTRODUCTION

Near bottom flow dynamics under waves is dependent on the state of flow regime in the bottom boundary layer. With the increase in free stream velocity, turbulent eddies start to appear in the neighborhood of the bottom and diffuse in the vertical direction. The turbulence mixing changes vertical velocity distribution and increases bottom shear stress, which subsequently causes bed-sediment transport. Identification of flow regime in the boundary layer under waves becomes very important from the viewpoint of the prediction of sediment transport phenomena. Consequently, there have been many studies to investigate the phenomena of flow transition under oscillatory motion. Most of these studies considered flow in the bottom boundary layer induced by regular sinusoidal oscillations in the free stream and have achieved a fairly good understanding on the mechanism of turbulence generation (Hino et al., 1976; Jensen et al., 1989: Eckmann and Grotberg,

1991; Foster et al., 1994 etc.).

Laminar-to-turbulent transition under waves first starts at decelerating phases prior to flow reversal. During decelerating phases, the reversal in near bottom flow velocities can be observed well before than that in the free stream, hence the vertical velocity profiles include inflection points. When the free stream velocity increases, the adverse pressure gradient at these phases becomes relatively large that causes shear instability in the vertical velocity profiles and results in the initiation of flow turbulence (Foster et al., 1994).

Flow transition for smooth bed condition under sinusoidal waves is conveniently defined based on a critical wave Reynolds number. Although the onset of turbulence generally varies over a range of Reynolds number and is dependent on individual experimental environments, based on experimental data, several researchers have put forward values of critical Reynolds numbers for sinusoidal waves. Following the definition of wave Reynolds number (Re) proposed by Jonsson (1966), the value generally suggested is around the critical Reynolds number, Re_{cr}, $=1.5\times10^5$ (Hino et al., 1976; Jensen et al., 1989; Eckmann and Grotberg, 1991; Akhavan et al., 1991 etc.). Hino et al. (1976) had observed unsteadiness of the flow at a much smaller Reynolds number; the fluctuations were of very small magnitude and did not significantly perturb the flow. It was also observed by Jensen et al. (1989) that although turbulence appeared in the decelerating phases at Reynolds numbers higher than the critical Re, the flow did not turn fully turbulent over the entire wave cycle until a very high Reynolds number, typically over $Re=1.0\times10^6$, is reached.

Under irregular waves, flow conditions vary over a wide range within a wave train. While some larger waves show turbulent behavior, there also exist smaller waves where flow could essentially be laminar. Wave irregularity thus introduces a wide range of pressure gradient condition, which subsequently would influence the transitional behavior. Unlike in the case of regular waves where flow transition starts at the critical Reynolds number, different behavior for laminar-to- turbulent and turbulent-to-laminar transitions is also expected under irregular wave trains.

In the present paper, flow transitional behavior under irregular oscillatory motions has been investigated through data from laboratory experiments. Detailed measurements of flow velocity in the bottom boundary layer have been performed. The data has been analyzed to study flow transition and to investigate the influence of irregularity on flow transition. The results show that under irregular oscillations the transition is not only governed by instantaneous flow properties, but also depends on flow conditions in preceding oscillations. As a result, distinct difference in behavior between laminar-to-turbulent and turbulent-to-laminar transitions has been observed. While much smaller oscillations show turbulent behavior when large turbulent motions precede these, initiation of turbulence is delayed in oscillations preceded by smaller laminar oscillations. The phenomenon has been termed as 'History effect' in this paper.

INSTRUMENTAL SET-UP AND EXPERIMENTAL PARAMETERS

Experimental System

The principle of the experimental system has been based on utilizing a servomotor at the core. The input piston signals, pre-obtained by generating free stream velocities of irregular wave, have been applied to drive the servomotor. Flow measurements then have been performed in a wind tunnel with 'air' as working fluid. The experimental system consists of two major components, a wave generation unit and a flow-measuring unit.

Details of the experimental system are presented in Fig.1. The wave generation unit was made up of signal control and processing components along with piston mechanism. The piston displacement signal has been fed into the instrument through a computer. Input signal, converted to corresponding analog data through a digital-analog converter, drives the servomotor. The piston mechanism has been mounted on a screw bar, which was connected to the servomotor. A motion in the servomotor thus generated motion in the piston. The feed-back on piston displacement, from one

instant to the next, has been obtained through a potentiometer that compared the position of the piston at every instant to that of the input signal, and subsequently adjusted the servomotor driver for position at the next instant. A smooth piston movement has been ensured by repeating the process until the end of the input signal has been reached.

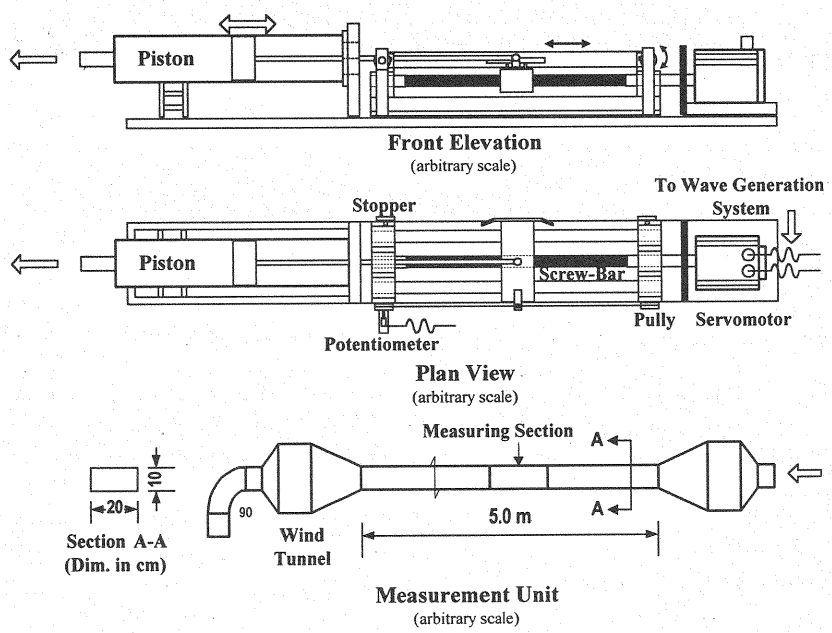

Fig.1 Description of experimental system

The flow measurement unit comprised of a wind tunnel and a one-component laser Doppler velocimeter (LDV) for flow measurement. The piston system has been connected to the wind tunnel through poly-vinyl chloride (PVC) pipes. The wind tunnel has dimensions of 5m in length, 20cm in width and 10cm in height, and was constructed from mirror-plane PVC plates on all four sides. Near the measuring section the sidewalls of the wind tunnel were made of transparent fiberglass sheets to facilitate LDV measurements. Finally, the LDV data has been stored in a computer and analyzed offline for ensemble average quantities.

Experimental Conditions

Piston displacement signal for an experiment has been derived from generated free stream velocity of irregular wave. Methodologies for the generation of irregular waves can be found in Samad and Tanaka (1999) and Samad (2000). A short segment of data containing about 10 waves has generally been selected from a long time series of generated free stream velocity. This was necessary to be able to complete one set of flow measurements within a time when a minimum change in surrounding experimental conditions could be maintained. The selection of the signal segment has been made in a way to represent widest possible flow conditions in a wave train. To facilitate computation of ensemble mean quantities, input piston signals have been run cyclically for at least 50 cycles. Both input and measured data have been specified at a frequency of 100 Hz. Flow velocities have been measured at about 20 elevations within the depth to the centerline of the wind tunnel (z_{cl}) and closely spaced near the bottom.

In the present paper, experimental data from the transitional and the turbulent cases have been

presented. The experimental conditions are shown in Table 1. Where $T_{1/3}$ and $U_{1/3}$ are significant period of oscillations and free stream velocity, respectively, ρ and ν are density and kinematic viscosity of air, respectively, and $Re_{1/3}$ is Reynolds number based on significant free stream velocity explained later in this section. Same shape of irregular wave input signal has been used for both the cases with piston displacement (D_p) multiplied by a factor for Case 2. The significant Reynolds number for Case 1 lies in the transitional range; whereas, for Case 2 large significant Reynolds number has been achieved, which indicates the presence of sufficiently higher level of turbulence.

Table 1 Experimental conditions

Cases	z_{cl} cm	$T_{1/3}$ s	ρ g cm^{-3}	ν cm^2 s^{-1}	$U_{1/3}$ cm s^{-1}	$Re_{1/3}$
Case 1	5.0	3.0	0.00122	0.147	242	1.9×10^5
Case 2			0.00119	0.152	507	8.1×10^5

Accuracy of Experimental System

The accuracy of the experimental system has been examined at various levels and the details of accuracy assessment of the system can be found in Tanaka et al. (2000). The primary one has been the comparison of input and ensemble average piston displacement (D_p) and free stream velocity (U). Fig.2 shows the comparison for Case 2. In the figure the piston displacement and free stream velocity have been normalized by the depth to the centerline of the wind tunnel (z_{cl}) and significant free stream velocity ($U_{1/3}$), respectively. A very high accuracy of the system in reproducing the input signal can be well observed from the figure.

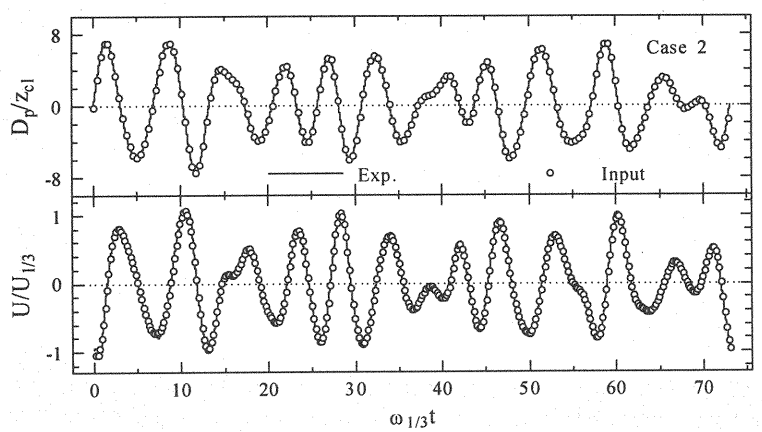

Fig. 2 Comparison of input and measured piston displacement and free stream velocity, Case 2

Considered Wave Reynolds Numbers

The irregular wave Reynolds number ($Re_{1/3}$) has been defined in terms of significant properties of oscillation and has been made analogous to wave Reynolds number defined (Re) by Jonsson (1966) for sinusoidal waves, such that:

$$Re_{1/3} = \frac{U_{1/3}^{\ 2}}{\nu\omega_{1/3}} \qquad (1)$$

where $\omega_{1/3}$ is significant frequency of oscillation given by $2\pi/T_{1/3}$.

In the present experiments, because of irregularity in oscillation shapes, it is expected that different waves in the train would show properties of all different flow regimes. To facilitate investigation of these changing flow properties, a half wave Reynolds number, Re_p, corresponding tothe half period (T_p) and the velocity peak (U_p) of oscillations:

$$Re_p = \frac{U_p^2 T_p}{\pi \nu} \tag{2}$$

has also been utilized. Fig.3 shows the variation of Re_p for both the cases along with corresponding free stream velocities. From the consideration of flow transition in sinusoidal motions, Case 1 shows that in most part of the train the flow mainly remain in laminar region, whereas, for Case 2, the half wave Reynolds numbers remain mostly in the turbulent zone with one or two segments of laminar motion.

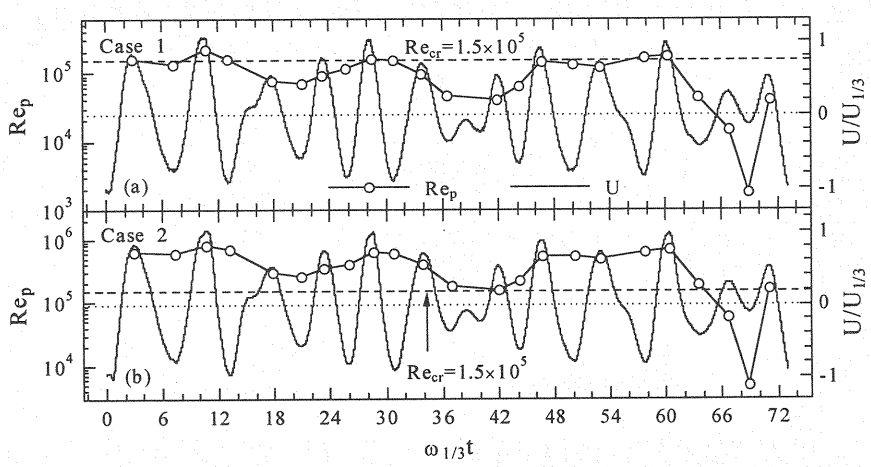

Fig. 3 Variation of half wave Reynolds numbers along with free stream velocity; Case 1 and (b) Case 2

VELOCITY PROFILES

Time Variation of Raw and Ensemble Average Velocities

Recorded raw velocities at selected elevations for Case 2 are presented in Fig.4. A wide range of flow situations can readily be identified from the figure. While some oscillations in the train with relatively higher magnitudes show very high turbulent intensities (marked with arrows), the turbulent energy is reduced in the presence of successive smaller oscillations.

The reduction in turbulent energy takes place gradually and needs the presence of several smaller oscillations to fully deplete the turbulent energy. As a result, oscillations those follow large turbulent motions, show properties of flow turbulence even if those have much smaller Reynolds numbers, in the laminar regime from sinusoidal wave consideration. One such motion is marked as '*A*' in the figure. On the other hand, several larger oscillations are required for sufficient build-up of the potential to initiate turbulence generation (marked as '*B*' in the figure). These are characteristic of flow transition under irregular oscillations and would be analyzed further in details.

Figures 5 and 6 show ensemble average velocities for both cases at selected elevations along with those from laminar solution. For Case 1 (Fig.5) flow over most of the domain shows good

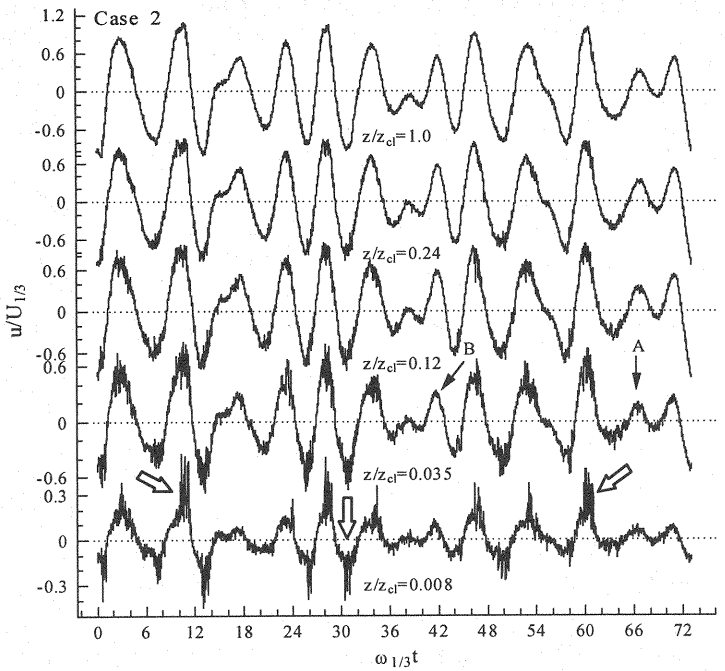

Fig. 4 Time variation of raw velocity records at selected elevation, Case 2

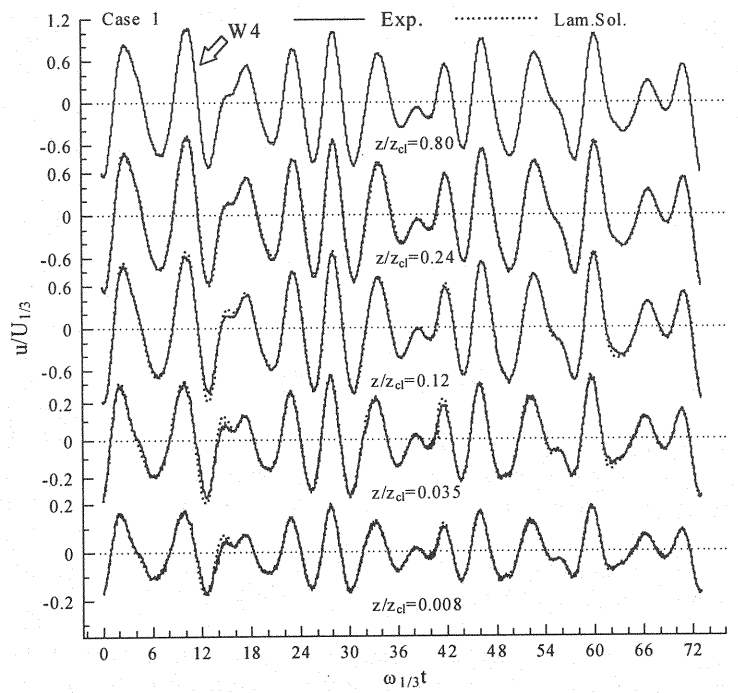

Fig. 5 Variation of ensemble average velocities along with corresponding laminar solution data, Case 1

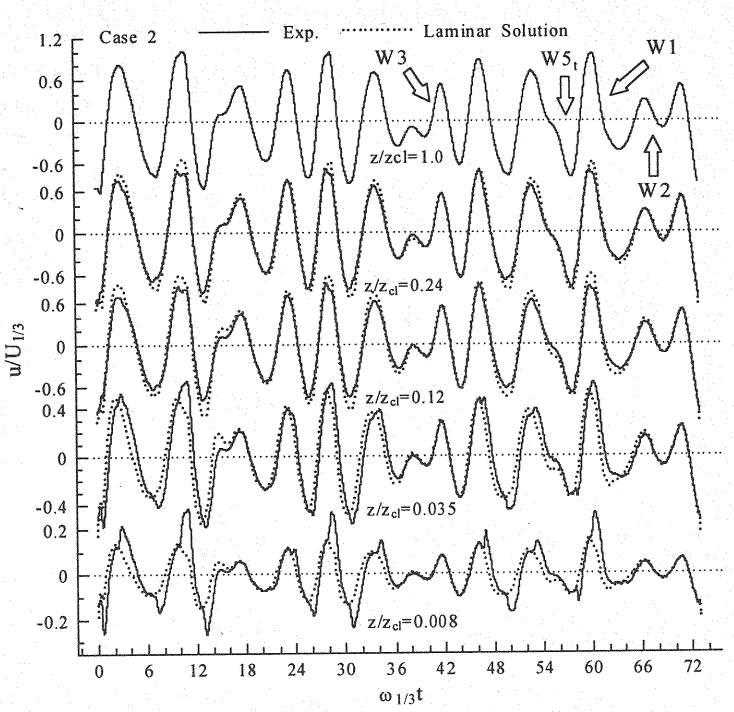

Fig. 6 Variation of ensemble average velocities along with corresponding laminar solution data, Case 1

agreement with laminar solution. Even at phases where relatively higher turbulent energy is present in raw velocity record (W4 in the figure), ensemble average velocity shows only a small difference with laminar solution data. This indicates that except for few oscillations, turbulence generated in Case 1 has much smaller magnitude to cause any significant mixing in the boundary layer.

For Case 2 (Fig.6), at phases where high turbulent intensities appeared, the ensemble-averaged velocities increase rapidly close to the bottom and are much higher in magnitude than corresponding laminar solution. But, moving away from the bottom, the ensemble-averaged velocities reduce suddenly. This is due to the momentum exchange by turbulent fluctuations that causes velocity acceleration close to and deceleration away from the bottom, which was first pointed out by Hino et al.(1976) under sinusoidal motions.

Oscillations marked as W1, W2 and W3 in this figure show characteristic behavior of turbulence carry-over and build-up, and have been discussed along with vertical velocity profiles in the following section. Half-oscillation trough marked as $W5_t$ in the figure shows the influence of smaller pressure gradient in an oscillation with very high half wave Reynolds number and would be discussed further later in connection with time averaged flow properties.

Vertical Profiles of Ensemble Averaged Velocities

Figure 7 shows the influence of turbulence carry-over on turbulent-to-laminar transition as reflected in vertical velocity profiles for W1 and W2. The high oscillation W1, at $\omega_{1/3}t$=59.0 for Case 2, has Re_p values corresponding to wave crest and trough as $Re_{p,crest}=6.97\times10^5$ and $Re_{p,trough}=1.92\times10^5$. This is followed by a much smaller oscillation W2 with $Re_{p,crest}=5.99\times10^4$ and $Re_{p,trough}=4.99\times10^3$. For the W1 the vertical velocity profiles show (Fig.7(a)) a large difference with corresponding

laminar profiles due to presence of very high turbulent intensities. The Reynolds numbers (Re_p) in the following oscillation W2 is very small; hence W2 represents flow in laminar condition from the consideration of sinusoidal motions. However, the velocity profiles in Fig.7(b) still show large differences from laminar solution. This indicates that W2 is still affected by the turbulence carried over from W1. Even very small Re_p under wave trough was not enough to completely diffuse the turbulent energy carried into this oscillation.

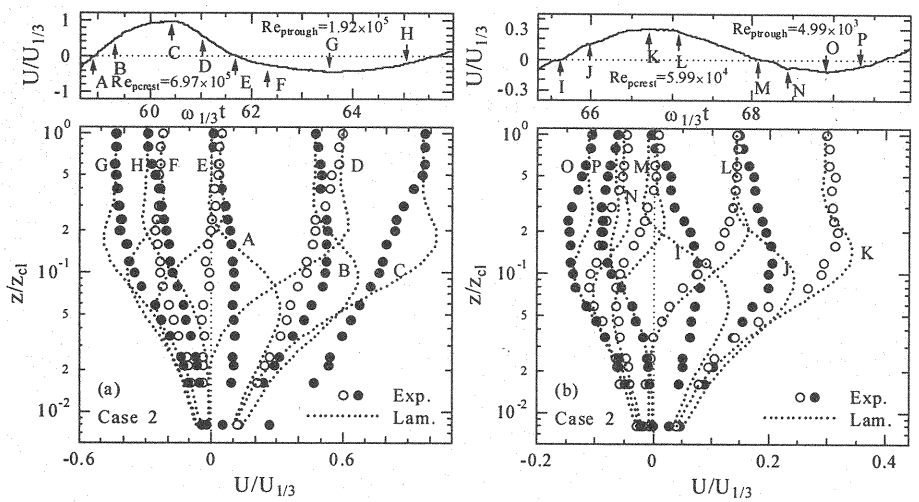

Fig. 7 Vertical velocity profiles at selected phases; (a) oscillation W1 and (b) W2, Case 2

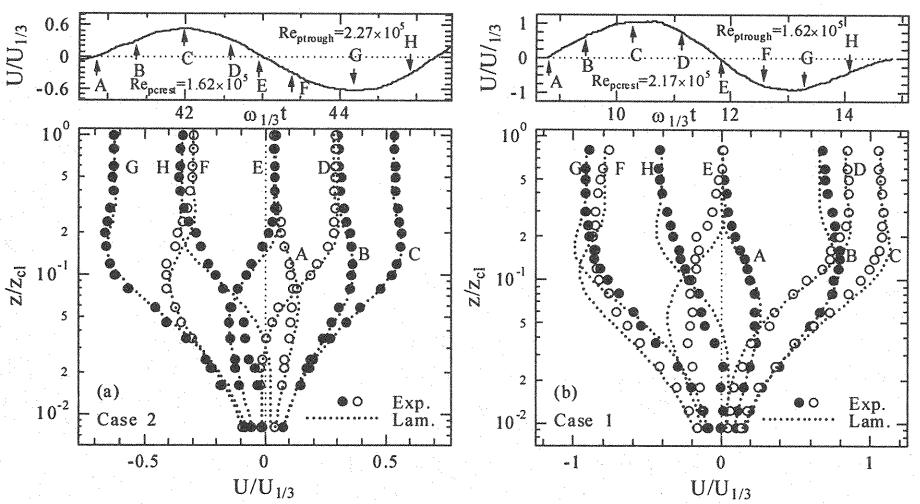

Fig. 8 Vertical velocity profiles at selected phases; (a) oscillation W3 (Case 2) and (b) W4 (Case 1)

On the other hand, the initiation of laminar-to-turbulent transition requires sufficient build-up of turbulent energy to produce traces of turbulence. Fig.8 shows vertical velocity distribution under W3 and W4 as marked in Figs. 6 and 5 respectively. W3 has Re_p values as $Re_{p,crest}$=1.62×10^5 and $Re_{p,trough}$=2.27×10^5. Although these Reynolds numbers are in the transitional range, the velocity

profiles show predominantly laminar behavior (Fig.8(a)). W4 has Re_p values are in the same range with W3 ($Re_{p,crest}$=2.17×10^5 and $Re_{p,trough}$=1.62×10^5), however, the vertical velocity profiles show sufficient difference from corresponding laminar profiles than those in W3 at almost all phases. The reason that W4 shows presence of turbulence is also related to the carry over of turbulent energy from the previous oscillation. Relatively higher $Re_{p,crest}$ in W4 initiated the generation of turbulence and that created a favorable condition for higher turbulence in the trough although $Re_{p,trough}$ was relatively smaller. Whereas the motion preceding W3 has smaller pressure gradient persistent for a longer period, allowing a complete dissipation of turbulent energy, as such almost no turbulence has been carried into W3.

This process of turbulence carry-over and build-up indicates that under irregular oscillation the state of flow at an instant is sometime governed by the conditions in the preceding oscillations. Because of this 'History Effect', turbulent-to-laminar and laminar-to-turbulent transitions show distinctly different behavior unlike that under sinusoidal motions. Although laminar-to-turbulent transition could be characterized similarly to that of sinusoidal waves, build-up of turbulent energy has been recognized to initiate the transition process. Turbulent-to-laminar transition, however, is much more affected by the process of carry-over of turbulent energy.

FLUCTUATING VELOCITIES AND TURBULENT INTENSITIES

Time variation of ensemble averaged root-mean-squared turbulent fluctuating velocity ($\sqrt{\overline{u'^2}}$) at a depth z/δ_f=1.60 from the bottom (where δ_f is the thickness of Stokes layer and given by $\delta_f=(2\nu/\omega_{1/3})^{0.5}$) is presented in Fig.9. The figure also shows the variation of free stream velocity and pressure gradient for both the cases. Under oscillatory motion, turbulence is first generated at decelerating phases. During acceleration, a favorable pressure gradient forces a reduction in the generation of turbulent energy. As a result, root-mean-squared fluctuating velocities show high peaks under decelerating phases. The magnitude of $\sqrt{\overline{u'^2}}$ is higher in Case 2, owing to higher $Re_{1/3}$ values, and shows the effect of turbulence carry-over in smaller oscillations (e.g., in W2). In Case 1, on the other hand, a gradual build-up in turbulent energy can be observed in the presence of successive higher oscillations (for $\omega_{1/3}t$=0.0 ~ 15.0, around W4). Prior to W3, a reduction in turbulent intensities can be observed in Case 2 due to the presence of smaller pressure gradinet and consequently W3 shows very small turbulent intensities as also observed in vertical velocity profiles.

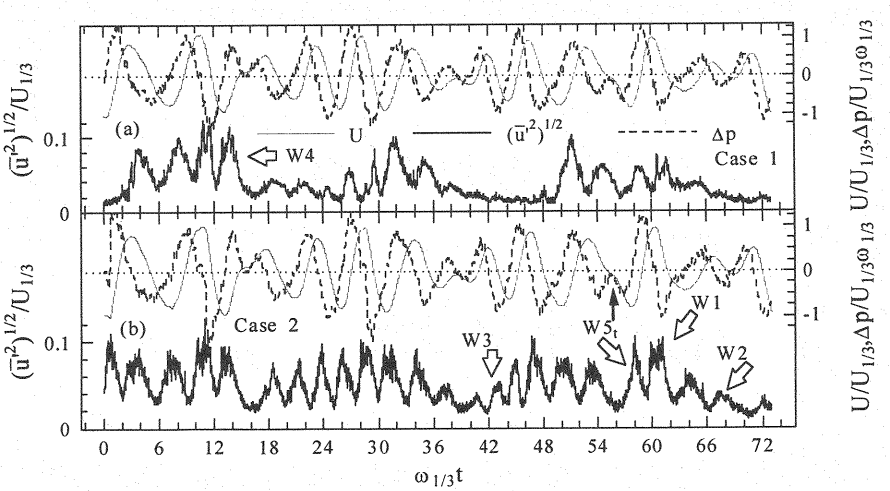

Fig. 9 Time variation of fluctuating velocities measured at z/δ_f=1.60 along with free stream velocities and pressure gradients; (a) Case 1 and (b) Case 2

Vertical variations of fluctuating velocities for W1 and W2 at phases marked in Fig.7 are shown in Figs.10 and 11. To indicate clearly the influence of turbulence carry-over into smaller oscillation W2, fluctuating velocities have been normalized by corresponding half wave velocity peaks. As turbulence is generated close to the bottom under decelerating phases, higher magnitude of fluctuating velocities can be observed near the bottom. During accelerating phases, turbulence generation reduces and it diffuses in the vertical direction with higher magnitude away from the bottom. Oscillation W1 (Fig.10) clearly shows such a behavior. But for W2 (Fig.11), although the relative magnitudes of normalized fluctuating velocities are much higher than those of W1, generation of turbulence can rarely be observed near the bottom. This implies that the turbulence present in W2 has not been generated by the oscillation itself rather carried into from W1.

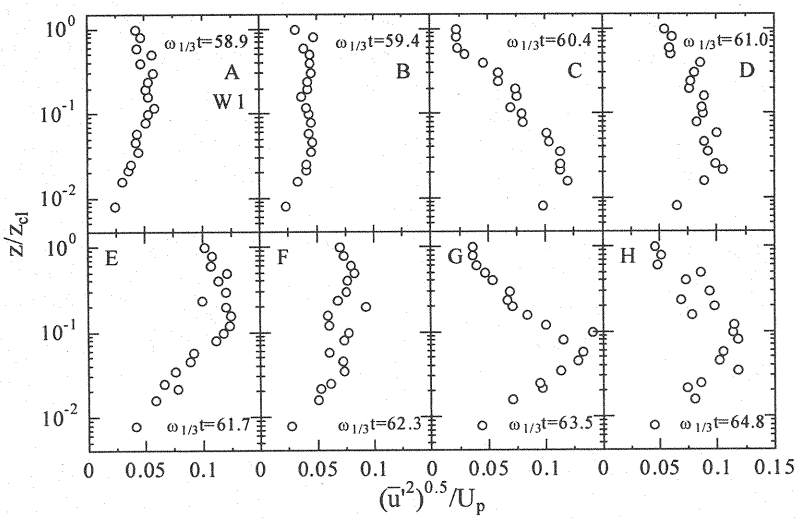

Fig. 10 Vertical profiles of fluctuating velocities, oscillation W1, Case 2

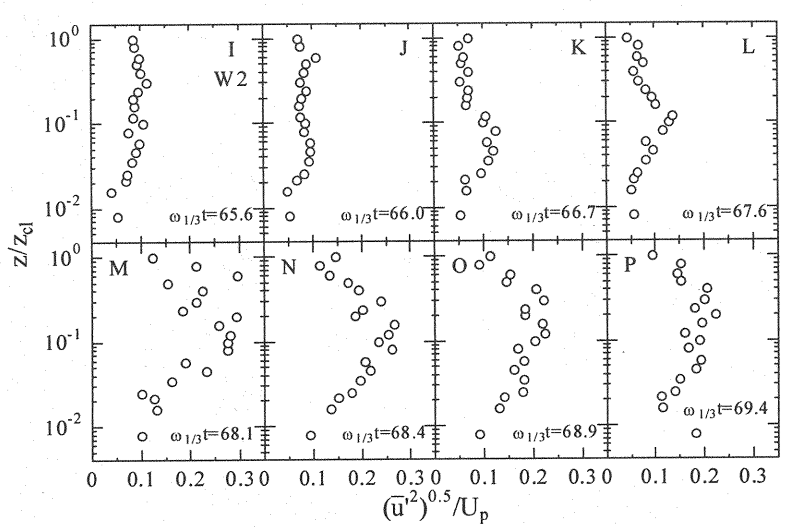

Fig. 11 Vertical profiles of fluctuating velocities, oscillation W2, Case 2

A comparison of time averaged fluctuating velocities ($\bar{\gamma}$) over half wave period at the same elevation, i.e., z/δ_f=1.60, has been made against those from sinusoidal motions (Fig.12). Under sinusoidal motions flow velocities have been measured in the boundary layer for different free stream velocity amplitudes with same period of oscillation. In the figure, averaged flcutuating velocities have been normalized by corresponding half wave peak velocity magnitudes. For laminar motion $\bar{\gamma}$ would ideally be zero and would increase with increasing turbulence, as has been observed for sinusoidal motions. Transition under sinusoidal motions can be observed to start at Re_p over 1.0×10^5, which is in very good agreement with the critical Reynolds number (Re_{cr}) as has been mentioned previously. At higher Reynolds numbers normalized averaged fluctuating velocities from both sinusoidal and irregular oscillations show good agreement, however, near the transitional range, a very high scatter in irregular oscillation data can be observed, which should be attributed mainly to History Effect (the oscillations W1 through W4 are also marked in the figure). Even in turbulent region, this History Effect can be observed in the stand out oscillation (wave trough $W5_t$ in the figure) with relatively lower magnitude of $\bar{\gamma}$. Oscillation $W5_t$ ($Re_{p,trough}=6.46\times10^5$) is also marked in Figs.6 and 9. During reversal in free stream velocity in this oscillation, smaller pressure gradient persisted over a longer time period (Fig.9). As such reduced generation of turbulent intensities resulted in a lower level of turbulence over the half oscillation.

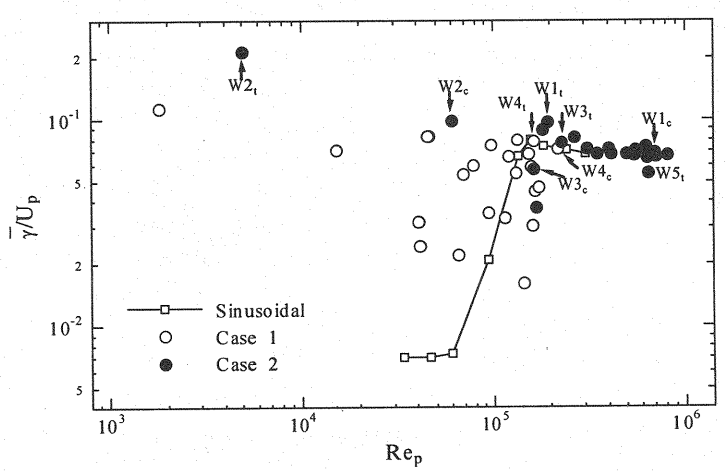

Fig. 12 Variation of fluctuating velocities averaged over half wave period at z/δ_f=1.60 against half wave Reynolds numbers

The phenomenon of History Effect to define turbulence carry-over could be ascribed to the irregularity in pressure gradient condition, which in turn, not only depends on the magnitudes of free stream velocity but also on its shapes. Even the presence of smaller pressure gradient over a longer period in a large oscillation would reduce generation of turbulent intensities as has been observed in $W5_t$. Conversely, the process of turbulence carry-over has particular significance when segments of smaller laminar oscillations are surrounded by large turbulent oscillations. For a wave train with very large significant Reynolds number ($Re_{1/3}$), such smaller oscillations would show fully turbulent properties.

OSCILLATORY FRICTION FACTOR

Transition to turbulence in oscillatory motion is conveniently defined through oscillatory friction factor diagram. Under laminar motion the solution to smooth bed friction factor (f_w) can be

obtained analytically. During flow transition, the friction factors deviate from laminar solution and in the turbulent state again show uniform trend. Also, for turbulent motion several relationships for oscillatory friction factor have so far been proposed (e.g., Fredsøe and Deigaard, 1992; Samad and Tanaka, 1999 etc.).

The influence of History Effect on friction factors under irregular oscillations has been studied from the factors computed from measured half wave properties. To calculate the friction factors, peak bottom shear stresses for corresponding half waves have been estimated by simultaneously fitting measured vertical velocity profiles in viscous and in logarithmic regions. Fig.13 shows the friction factor diagram based on half wave properties. Considerable overlap in flow regimes can be observed in the figure such that transition varies over a much higher range of Reynolds numbers. In turbulent region, the effect of smaller pressure gradient on turbulent intensities can also be observed in $W5_t$ with much reduced friction factor similar to that observed in Fig.12. Such that, the friction factor diagram alone is not sufficient to describe the state of flow regime present under irregular oscillations.

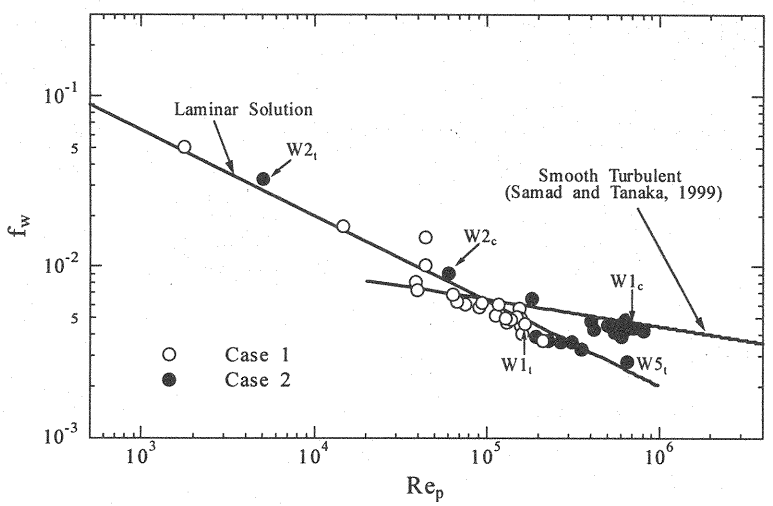

Fig. 13 Friction factor diagram corresponding to half wave Reynolds numbers

CONCLUSIONS

The process of flow transition in the bottom boundary layer under irregular oscillations for plane bed condition has been investigated through laboratory data. Experiments have been carried out in a wind tunnel with flow driven by a servomotor-based system.

It has been observed that the state of flow under irregular oscillations is not only governed by instantaneous flow properties, but also depends on the conditions in preceding oscillations. Because of this History Effect, distinctly different behavior can be observed for laminar-to-turbulent and turbulent-to-laminar transitions unlike those under sinusoidal motions.

Although laminar-to-turbulent transition was somewhat less influenced by the History Effect, need for turbulent build-up has been well identified with the delay of the initiation of turbulence until a sufficiently larger Reynolds number has been achieved. Turbulent-to-laminar transition, on the other hand, was much more influenced by the carry-over of turbulent energy from previous oscillations and varied over a very wide range of Reynolds numbers. Such that, the use of conventional flow transitional criteria based on sinusoidal wave friction factor diagram becomes unsuited to define flow transition under irregular oscillations.

ACKNOWLEDGEMENT

The authors express their sincere appreciation to The Scandinavia-Japan Sasakawa Foundation (No.00-18) for partially supporting the study.

REFERENCES

1. Akhavan, R., R.D. Kamm and A.H. Shapiro : An investigation of transition to turbulence in bounded oscillatory Stokes flows, Part I. Experiments, J. Fluid Mech., Vol.225, pp.395-422, 1991.
2. Eckmann, D.M. and J.B. Grotberg : Experiments on transition to turbulence in oscillatory pipe flow, J. Fluid Mech., Vol.222, pp.329-350, 1991.
3. Foster, D.L., R.A. Holman and R.A. Beach : Sediment suspension events and shear instabilities in the bottom boundary layer. Proc. Coastal Dynamics'94, pp.712-726, 1994.
4. Fredsøe, J. and R. Deigaard : Mechanics of Coastal Sediment Transport, World Scientific, 369p., 1992.
5. Hino, M., M. Sawamoto and S. Takasu : Experiments on transition to turbulence in an oscillatory pipe flow, J. Fluid Mech., Vol.75, pp.193-207, 1976.
6. Jensen, B.L., B.M. Sumer and J. Fredsøe : Turbulent oscillatory boundary layer at high Reynolds numbers, J. Fluid Mech., Vol.206, pp.265-297, 1989.
7. Jonsson, I.G. : Wave boundary layers and wave friction factors, Proc. 10th Int. Conf. Coastal Eng., pp.127-148, 1966.
8. Samad, M.A. and H. Tanaka : Estimating instantaneous turbulent bottom shear stress under irregular waves, J. Hydrosc. and Hydraulic Engg., JSCE, Vol.17, No.2, pp.107-126, 1999.
9. Samad, M.A.: Investigation of Bottom Boundary Layer Under Irregular Waves, Ph.D. Diss., Tohoku Univ., 148p., 2000.
10. Tanaka, H., Samad, M.A. and Yamaji, H. : Velocity measurements in an oscillatory boundary layer under irregular waves, Stochastic Hydraulics 2000, IAHR, Eds. Z.Y. Wang and S.X. Hu, A.A. Balkema, pp. 737-745, 2000.

APPENDIX – NOTATIONS

The following symbols are used in this paper:

D_p = piston displacement;

f_w = wave friction factor;

Re = wave Reynolds number;

$Re_{1/3}$ = irregular wave Reynolds number corresponding to significant properties;

Re_p = Reynolds number corresponding to half wave period and velocity peak;

t = time;

$T_{1/3}$ = significant wave period;

T_p = half wave period;

U = free stream velocity;

$U_{1/3}$ = significant free stream velocity;

U_p = magnitude of half wave velocity peak;

$\sqrt{\overline{u'^2}}$ = turbulent fluctuating velocity;

z = depth from the bottom of the wind tunnel;

z_{cl} = depth from the bottom to the centerline of the wind tunnel;

δ_l = Stokes layer thickness;

$\overline{\gamma}$ = fluctuating velocity time averaged over half wave period;

ν = kinematic viscosity of air;

ρ = mass density of air;

$\omega_{1/3}$ = wave frequency corresponding to significant wave period; and

ω_p = wave frequency corresponding to half wave period.

(Received July 2, 2000 ; revised October 2, 2000)